10-2-2023

State Space Modeling and Estimation of Flexible Structure Using the Theory of Functional Connections

Carlo Lombardi

Riccardo Bevilacqua

IAC-23-C2,3,6,x76965

State Space Modeling and Estimation of Flexible Structure Using the Theory of Functional Connections

Carlo Lombardi[a]*, Riccardo Bevilacqua[a]

[a] *Department of Aerospace Engineering, Embry-Riddle Aeronautical University, 1 Aerospace Boulevard, Daytona Beach, FL, 32114, USA*

* Corresponding Author

Abstract

In this work, we present a novel method to model the dynamics of a continuous structure based on measurements taken at discrete points. The method is conceived to provide new instruments to address the problem of flexible dynamics modeling in a spacecraft, where an effective mathematical representation of the non-rigid behavior of the is of critical importance in the design of an effective and reliable attitude estimation and control system. Both the measurements and the model that describes the structure can be affected by uncertainty. The purpose of the developed method is to estimate the position and the velocity of any point of the physical domain relying on a limited number of measurements while filtering out the noise. To this aim, the well-assessed Kalman filter is used in synergy with the recently developed Theory of Functional Connections (TFC). This is a mathematical framework to perform functional interpolation with applications in many fields being currently discovered and investigated. Initially, an algorithm for the solution of the corresponding static problem was developed based on the TFC; the results of the tests were promising and the approach presented in this work constitutes an effort to extend the idea to the dynamic case. In the proposed method, the continuous structure is approximated by the TFC constrained expression, while the system state variables are defined as the coefficients used to represent the free function in a basis of orthogonal polynomials. This leads to a system that, despite being continuous and thus formed of an infinite number of material points, is modeled using a finite number of state variables allowing for the use of Kalman filter to deal with the uncertainties intrinsic in both the modeling and measurements. This is accomplished by exploiting the original structure model Differential Equation(s) to obtain a process model for the filter and using the constrained expression itself as the measurement model. Then the Kalman filter algorithm is applied and the a posteriori estimates of the state variables (that is the free function coefficients) can be used to build the TFC expression that approximates the instantaneous shape of the structure, thus enabling the evaluation of the displacement at any point of the domain. The power of the proposed method is twofold. First, an estimate of the displacements of all the points is obtained based on a limited number of noisy measurements. Second, the relation between discrete measurements and continuous displacement field always accounts for the real physics of the problem. In this paper, the theoretical developments of the proposed approach are shown along with the results of numerical simulations showing the effectiveness of the method in estimating the actual dynamics of a Euler-Bernoulli beam. The technique yielded good results both for the free response and in the case of a forcing input to the system.

Keywords: Theory of Functional Connections, Flexible Dynamics, Kalman Filter, Structure Dynamics, Dynamic Modeling

Nomenclature

L	=	beam length
ρ	=	beam material mass density
A_s	=	beam cross-section area
E	=	beam material Young modulus
I	=	beam cross-section area moment of inertia
x	=	position of a beam element along the undeformed beam axis
y	=	displacement of the beam element relative to the undeformed condition
p	=	load distribution acting on the beam
ξ_i	=	free function expansion coefficients $(i = 1,2, \dots, n_b)$
n_c	=	number of constraints
n_b	=	number of basis functions used to expand the free function
n_s	=	number of measurement points along the beam
$\bar{q}$	=	generalized coordinates vector
T	=	number of samples to train the Kalman Filter covariance matrices
$(\cdot)_x$	=	differentiation with respect to the x variable
$\dot{(\cdot)}$	=	differentiation with respect to time

Acronyms/Abbreviations

TFC	:	Theory of Functional Connections
ODE	:	Ordinary Differential Equation
PDE	:	Ordinary Differential Equation
KF	:	Kalman Filter

EKF : Extended Kalman Filter
UKF : Unscented Kalman Filter

1. Introduction

The modeling and control of flexible structures is a very current topic in aerospace engineering research. This happens because, even though the rigid body assumption remains a very convenient option to model the dynamics of some space vehicles and to make some pre-design evaluations, the highly flexible behavior shown by many modern spacecrafts requires more accurate models that are capable to effectively portray this type of dynamics. One of the factors behind the strongly flexible behavior that many space vehicles tend to exhibit can be traced back to the great effort that aerospace engineers spend trying to reduce both the weights and the size of the spacecrafts by using lightweight and less rigid structural solutions as well as folding mechanisms to reduce the stowed size of large appendages. Moreover, some elements of critical importance for the success of a space mission are naturally prone to exhibit flexible behavior because of their shapes: very common and important examples are solar arrays and antennas [1] which, from a structural modeling point of view, can be represented as thin plates and beams. On top of this, spacecrafts committed to some particular missions (e.g., very long-range astronomical observation) are often subject to attitude control requirements that may be very stringent in terms of both accuracy and responsiveness.

In general, the problem of the dynamics of flexible structure has been investigated extensively throughout the history of engineering, and not only in the specific field of space flight.

A very general classification of the methods to model the dynamics of continuous elastic bodies that were developed through the years involves two main groups: the infinite-dimensional models and the finite-dimensional models. In this review, we start focusing on the first class of methods and then we are going to move to the second one, which is of greater interest for the developments presented in this work. Introducing the first group, we can very concisely say that the infinite-dimensional models result from the direct application of the continuum mechanics physics and are characterized, in their mathematical description, by the presence of Partial Differential Equations (PDEs); very simple examples are the classic Euler-Bernoulli beam theory and the Kirchhoff-Love theory for the thin plate, but more advanced theory can be used as well [2]. When describing the complete dynamics of a spacecraft, where usually parts that can be treated as rigid bodies interact with flexible elements, this leads to hybrid systems of PDEs and Ordinary Differential Equations (ODEs) [3]. This type of models, despite being rigorous, introduce non-negligible complexity in both control and estimation of the state of these systems. Several methods were developed in the years [4] and to this day this is still an active research field, opening to the adoption of machine learning techniques [5] [6].

The idea of approximating the space-continuous system using a finite number of spatial coordinates gave birth to the finite-dimensional methods. The techniques belonging to this group share the feature of producing simpler representations of the system dynamics in the form of generally coupled ODEs, which can be conveniently treated using the theory of dynamical systems. In this way, using the finite-dimensional approach, the system control and estimation tasks can be carried out exploiting the well-assessed and widely developed theory that exists for this kind of systems. Despite these aspects that are common to all the methods belonging to this class, the way the result is achieved widely differs among the techniques with significant impacts on complexity, efficiency and versatility. Here we just want to provide a summary of the most important sub-families of available methods. The first group is represented by the so-called lumped parameter representations. In this kind of method, a flexible-rigid system of any complexity is subdivided into a number of elements that are assumed to be perfectly rigid bodies; then, these bodies are constrained to each other by mathematical relations that aim to reproduce the mechanical characteristics of the constitutive material. An approach that allows to obtain a more accurate approximation at the cost of a generally higher complexity is the Finite Element Method [7], [8], [9], [10]. In this case, the whole structure is still subdivided into a number of smaller elements, but at this time they are not assumed to be perfectly rigid and their flexible behavior is described using the results from the classic structural theories (like the beam theory for 1-dimensional structure or plate theory for 2-dimensional structures).
Finally, a different approach is the assumed (or synthetic) modes representation where, following a procedure similar to the analytical modal analysis, the structure dynamical response is decomposed in terms of a weighted sum of space-continuous functions in which the weights are assumed to be time-dependent) [11]. One of the main drawbacks of this approach resides in the choice of the synthetic modes that must satisfy the geometric constraints and possibly they should ensure good convergence properties; the achievement of both these characteristics at once can be nontrivial in some cases and may require a nonnegligible pre-design effort.

A problem that is central in this work is the development of a model for the dynamics of flexible structures and its use to perform state estimation. In fact, it is well known that the task of estimating the actual state of a system based on a number of noisy measurements

can represent a challenge in many situations. Several methods to produce reasonably accurate estimates, trying to eliminate the error component introduced during the measurement process have been developed based on statistical approaches. In particular, a very effective and deservedly popular technique used to reach this goal is the Kalman filter [12] [13], which constitutes a very powerful and, thanks to its many variants like EKF and UKF [14] [15], versatile instrument to perform statistical error filtering on a collection of noisy measurements. A very important element of the Kalman filter is the dynamical model of the system whose states are to be estimated. The classic development of the Kalman filter is based on finite-dimensional models with a finite number of states, while structural elements, being continuous systems, have an infinite number of states (e.g., position and velocity of all the points in a beam); an infinite-dimensional extension of the classic linear Kalman filter was proposed in the 1970s [16] and only recently some interesting advancements were obtained for linear time-varying [17] and nonlinear systems [18]; anyway, the techniques can be quite complex to implement requiring more advanced concepts like an effective definition (and estimation for real-world applications) of space-continuous noise distributions. Another issue with dealing with a fully continuous model description consists in the limited availability of measurements: in some cases, it is possible to have a very dense observation sampling of the target structure, but this is not always the case depending on the choice of the sensors and on space, weight and possible budget limitations. In general, the availability of a limited number of measurements should be taken into account. All the factors mentioned above suggest using a finite-dimensional Kalman filter where possible. In this regard, some of the above-mentioned finite-dimensional models could be used in for the prediction part of the filter, but what we want to present in this paper is a novel approach that aims to overcome the drawbacks highlighted for the other techniques. For this purpose, the recently developed mathematical framework called the Theory of Functional Connections (TFC from now on) is used to approximate the deformed shape of the structure subject to a set of constraints and external loads. The proposed approach exploits the versatility of the TFC to provide a highly flexible and general solution to the problem of modeling the dynamics of flexible structures. Moreover, the models obtainable following this technique are capable of yielding finite-dimensional approximations of the behavior of continuous structures without introducing an actual discretization of the system. This aspect, together with the moderate number of state variables usually required, makes this approach accurate and computationally efficient at once.

This paper is organized as follows: in section 2 the key concepts of the Theory of Functional Connections are briefly presented along with a short review of the linear Kalman filter. Section 3 describes the theoretical development of the flexible structure dynamic model and its implementation in the Kalman filter framework for improving the state estimation. In section 4 the numerical simulation setup is described and the results of the tests are discussed, while in section 5 the main conclusions are reported and further developments are proposed.

2. Preliminaries

In this section, we want to provide a synthetic review of the two main mathematical tools that will be used in the rest of this paper to develop the proposed methodology: the Theory of the Functional Connections and the Kalman Filter.

2.1. Theory of Functional Connections

The Theory of Functional Connections (TFC) [19] is a recently developed mathematical framework performing linear functional interpolation. The theory, which has been introduced in [20] for univariate and extended to multivariate in [21], generalizes interpolation by deriving analytical functionals representing all possible functions subject to a set of linear constraints. TFC has been developed for n-dimensional rectangular domains subject to the absolute, derivative, integral, component, infinite, and any linear combination of these constraints [22], [23]. The functional expression representing the whole family of functions satisfying a given set of n_c constraints is called *constrained expression* and can be formally written in one of these two forms:

$$y\big(x, g(x)\big) = g(x) + \sum_{i=1}^{n_c} \eta_i\big(x, g(x)\big)\, s_i(x) \qquad (1)$$

$$y\big(x, g(x)\big) = g(x) + \sum_{i=1}^{n_c} \rho_i\big(x, g(x)\big)\, \Phi_i\big(x, s(x)\big) \qquad (2)$$

In the first formulation, $s_i(x)$ is a set of n_c linearly independent *support functions*, while $\eta_i\big(x, g(x)\big)$ are coefficient functionals that, in the particular case of univariate interpolation, reduce to simple constants.

In the second formulation, $\Phi_i\big(x, s(x)\big)$ are *switching functions*, i.e. special functions that can be obtained as linear combinations of the support function, each one with the property of being equal to 1 at the corresponding constraint and zero at all the other constraint nodes. $\rho_i\big(x, g(x)\big)$ are the *projection functionals* and are obtained by rewriting the constraint equations in terms of the $g(x)$ function (i.e., they represent the constraints written in terms of $g(x)$).

In both the expressions, $g(x)$ is called the *free function* and, as the name suggests, can be freely chosen

as long as it is defined at *all* the constraint points. In spite of this being the only condition required to $g(x)$ to be part of the constrained expression, we will see that in some applications (and for some representations of $g(x)$) additional requirements could be necessary.

The mathematical meaning of the constrained expression shown above (regardless of the chosen representation) is a functional projecting the whole space of functions to just the subspace fully satisfying the constraints. This way, constrained optimization problems, such as differential equations, can be transformed into unconstrained problems, and consequently, be solved using simpler, faster, and more robust and accurate methods.

2.2. Kalman Filter Review

In this subsection a short review of the Kalman filter fundamentals is presented. The great popularity of the Kalman filter is attributed to it being a highly effective and computationally efficient way to improve the state estimation of a system in the presence of nonnegligible measurement noise. The filter can be exploited in diverse ways and several extensions and variants have developed over the years since the filter was first introduced in 1960 by Rudolf E. Kálmán [12]. In this research, we focus on the original linear development proposed by Kálmán.

Before showing the main formulas of the Kalman filter, we want to specify that in this section for illustrative reasons we are going to refer to a linear dynamic system subject to n_i inputs and whose state is fully characterized by n_s state variables. Moreover, we consider a measurement system providing n_m outputs which are linear combinations of the system state variables.

Let us consider the discrete-time linear dynamic system subject to noise:

$$\bar{x}_{k+1} = \hat{A}_k \bar{x}_k + \hat{B}_k \bar{u}_k + \bar{w}_{k+1} \tag{3}$$

where $\bar{w}_{k+1}$ is the process noise term that is used to model the uncertainty in the mathematical representation of the dynamics, $\hat{A}_k$ and $\hat{B}_k$ are the matrices characterizing the discrete-time dynamics of the system. In the framework of the Kalman filter, the process noise is assumed to have a zero-mean normal distribution characterized by a $n_s \times n_s$ covariance matrix denoted by Q and is also assumed to not be time-correlated (i.e., $[\bar{w}_1, \cdots, \bar{w}_k]$ are stochastically independent).

For the output of the system, the measurement equation is:

$$\bar{y}_{k+1} = H\bar{x}_{k+1} + \bar{v}_{k+1} \tag{4}$$

Here, H is the $n_m \times n_s$ matrix representing the linear operator mapping from the state space to the observable space and $\bar{v}_{k+1}$ is the measurement noise term with the same assumptions as the process noise, but with a $n_m \times n_m$ covariance matrix denoted by R.

The $n_s \times n_s$ covariance matrix characterizing the uncertainty on the estimate of the state of the system is denoted by P.

The Kalman filter update equation is the following:

$$\bar{x}_{k+1}^{+} = \bar{x}_{k+1}^{-} + K_{k+1}\bar{y}_{k+1} \tag{5}$$

where the $^-$ and $^+$ superscripts denote the a priori and the a posteriori estimates, respectively, and K_{k+1} is the Kalman gain. The Q and R covariance matrices can be considered as constants in many practical cases, and so we will do in the developments of this paper. For the convenience of the reader, the key formulas for the linear Kalman filter are summarized in Table 1.

Table 1 - A summary of the Kalman filter main formulas.

PREDICTION	
Predicted state estimate	$\bar{x}_{k+1}^{-} = \hat{A}_k \bar{x}_i^{+} + \hat{B}_k \bar{u}_k$
Predicted state estimate covariance	$P_{k+1}^{-} = \hat{A}_k P_k^{+} \hat{A}_k^T + Q$
CORRECTION	
Innovation residual	$\bar{z}_{k+1} = \bar{y}_{k+1} - H\bar{x}_{k+1}^{-}$
Innovation covariance	$S_{k+1} = HP_{k+1}^{-}H^T + R$
Kalman gain	$K = P_{k+1}^{-}H^T S_{k+1}^{-1}$
A posteriori state estimate	$\bar{x}_{k+1}^{+} = \bar{x}_{k+1}^{-} + K\bar{z}_{k+1}$
A posteriori state estimate covariance	$P_{k+1}^{+} = (I - KH)P_{k+1}^{-}$

3. System Modeling and Filter Design

In this section, the approach taken to model structural dynamics using the tools provided by TFC and the Kalman filter is presented in two subsections. The first subsection shows the derivation of a TFC-based structural dynamics model. In the second subsection, the resulting finite-dimensional model is integrated into a classical Kalman filter implementation so to exploit the simplicity and effectiveness of this mathematical tool in dealing with the estimation of the state of a dynamical system: once the estimates are produced for the TFC-based finite-dimensional representation, the deformed shape of the true continuous structure can be easily reconstructed exploiting the TFC constrained expression.

While we strive to keep the discussion as general as possible, a specific type of structure has been chosen to allow numerical verification to be performed. For clarity, a simple example is used in the following derivations. This allows us to focus on important aspects of the theoretical development without adding complexity that might interfere with the true purpose of the derivation.

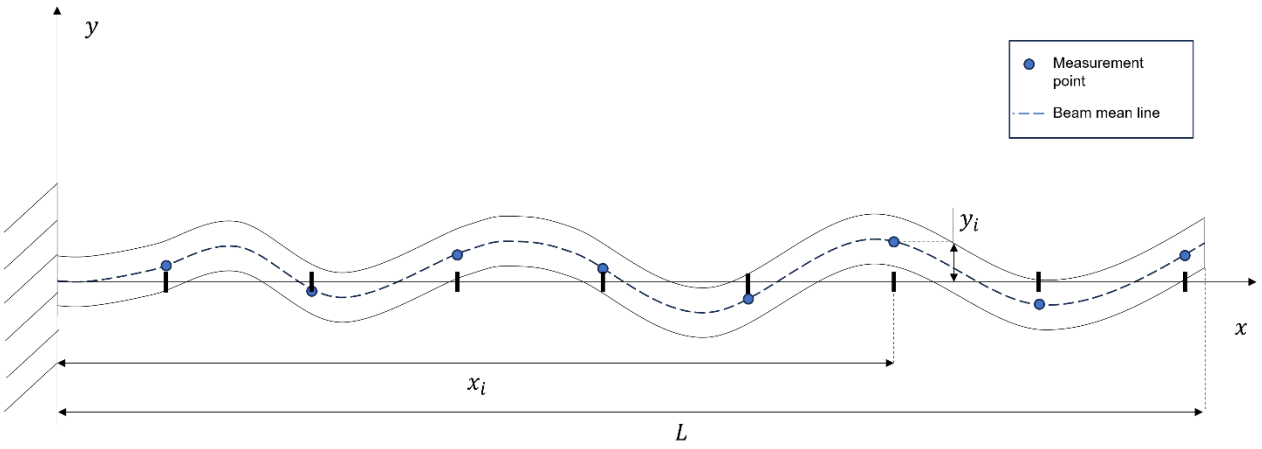

Figure 1 – Beam geometry and coordinate system

Nevertheless, this does not affect the generality of the ideas presented in this paper, making the approach suitable to be extended to more complex systems at the cost of a longer derivation. The structural problem that will be addressed in the subsequent sections is the problem of modeling and estimation of the dynamics of a Euler-Bernoulli cantilever beam (Figure 1), whose fundamental equation is reported here:

$$\rho A_s \frac{\partial^2}{\partial t^2} y\big(x, g(x,t)\big) + \frac{\partial^2}{\partial x^2}\left(EI \frac{\partial^2}{\partial x^2} y\big(x, g(x,t)\big)\right) = q(x,t) \quad (6)$$

With E being the Young modulus, ρ the beam material density, A_s the cross-sectional area and I the cross-section area moment of inertia.

3.1. TFC-based Dynamic Model

In the following, we are going to derive the dynamic model describing the behavior of the vibrating beam using the tools provided by the TFC: this will allow to obtain a finite-dimensional and linear representation of the original infinite-dimensional system, thus enabling the use of a classic linear Kalman filter to solve the problem of state estimation in the presence of measurement errors.

The first step in the process consists in the derivation of the constrained expression for the problem under consideration. In this specific case, we are going to simply consider the traditional problem of a cantilever beam, which mathematically translates into a boundary values problem. Nevertheless, it is worth to recall that the TFC allows to consider a wide variety of conditions, including any linear constraint and even some nonlinear constraints [19]. Moreover, the fact that these conditions can be imposed at any point of the domain, and not only at the boundaries, makes the TFC a very powerful tool, capable of overcoming some of the limitations of the classic differential equation theories.

In order to derive the constrained expression according to the formulation in equation (1), we need as many linearly independent support functions as the number of the constraints. These functions can be freely chosen, the only limitation being the above-mentioned linear independence at the constraint points.

In our case, the constraints to be imposed represent the simple boundary conditions of a cantilever beam of length L:

$$\begin{cases} y\big(0, g(0)\big) = 0 \\ \dfrac{d}{dx} y\big(0, g(0)\big) = 0 \\ \dfrac{d^2}{dx^2} y\big(L, g(L)\big) = 0 \\ \dfrac{d^3}{dx^3} y\big(L, g(L)\big) = 0 \end{cases} \qquad x \in [0, L]$$

A good set of support functions that satisfies the linear independence requirement for this problem is the following:

$$s_1(x) = 1 \qquad s_2(x) = x \qquad s_3(x) = x^2 \qquad s_4(x) = x^3$$

The resulting constrained expression has the form:

$$y\big(x, g(x)\big) = g(x) - g(0) - g_x(0)x + \left(\frac{L}{2} g_{xxx}(L) - \frac{1}{2} g_{xx}(L)\right) x^2 - \frac{1}{6} g_{xxx}(L) x^3 \quad (7)$$

The free function $g(x)$ can be expressed in a basis of orthogonal functions:

$$g(x) = \sum_{j=1}^{n_b} \xi_j h_j\big(z(x)\big) \tag{8}$$

where n_b denotes the number of function bases $h_j(x)$ to be used and $z(x)$ is a function mapping from the physical domain (in the case of the beam $x \in [0, L]$) to the domain of the orthogonal functions, which is generally different. In this work, we are going to expand $g(x)$ in term of Chebyshev polynomials, whose domain is $z \in [-1,1]$. Thus, the map $z(x)$ is:

$$z(x) = \frac{2x}{L} - 1 \tag{9}$$

Considering the full expansion of $g(x)$ (i.e., for $n_b = \infty$) substituted into (9), letting the ξ_j coefficients vary will give the entire function space projected onto the considered set of conditions. Using a finite subset of orthogonal functions is an approximation, but it still provides good results even when n_b is relatively small.

The TFC-based finite dimensional dynamical model of the structure can be obtained by considering ξ_j coefficients as functions of time and substituting (8) into (7) and the resulting expression into the Euler-Bernoulli beam equation (6) . Finally, the TFC-based finite dimensional dynamical model of the structure can be obtained by imposing the differential expression at some sampling points along the beam (the best choice consists in those locations where the measurements are available).

If we consider a beam with a constant cross-section and made of homogeneous material, such that both E and I are independent of the x position along the beam axis, we can take advantage of some simplifications obtaining the following set of linear ODEs in matrix form:

$$M\ddot{\bar{\xi}}(t) + K\bar{\xi}(t) = \bar{q}(t) \tag{10}$$

In the above expression, $\bar{q}(t)$ is a $n_c \times 1$ vector obtained discretizing the continuous load distribution $q(x,t)$ in equation(6). M and K are $n_c \times n_b$ in the form:

$$M = \rho A_s \begin{bmatrix} \big(\bar{f}(x_1) + \bar{a}\big)^T \\ \big(\bar{f}(x_2) + \bar{a}\big)^T \\ \vdots \\ \big(\bar{f}(x_{n_c}) + \bar{a}\big)^T \end{bmatrix}$$

$$K = EI \begin{bmatrix} \beta^4 \bar{h}^{T''''}\big(z(x_1)\big) \\ \beta^4 \bar{h}^{T''''}\big(z(x_2)\big) \\ \vdots \\ \beta^4 \bar{h}^{T''''}\Big(z\big(x_{n_c}\big)\Big) \end{bmatrix}$$

The $\bar{f}(x)$ and $\bar{a}$ terms above were introduced for compactness and are defined as follows:

$$\bar{a} = -\bar{h}\big(z(0)\big)$$

$$\bar{f}(x) = \bar{h}\big(z(x)\big) - \beta\bar{h}'\big(z(0)\big)x + \Big(\frac{L}{2}\beta^3\bar{h}'''\big(z(L)\big) + -\frac{1}{2}\beta^2\bar{h}''\big(z(L)\big)\Big)x^2 \; -\frac{1}{6}\beta^3\bar{h}'''\big(z(L)\big)x^3$$

Finally, β denotes the derivative of the function mapping from the physical domain of the structure to the domain of the function bases. Since for the developments shown in this work the free function is expanded in terms of Chebyshev polynomials, the map (9) is linear and consequently the β term is constant:

$$\beta = \frac{dz}{dx} = constant$$

At this point, the following final observations are important:

- The number of function bases n_b used to represent the free function and the number of points n_c at which the dynamic equation is applied can be freely chosen, but this is subject to some restrictions. In fact, in the context of the applications considered in this paper, n_c depends on the availability of measurements along the physical beam: in general, due to weight, budget and technological limitations, the number of locations at which the beam displacement is measured can be limited. On the other side, the number of function bases that can be used is virtually unbounded and can be chosen at discretion of the user. Nevertheless, in order for the system to work efficiently, n_b cannot be too big because of 2 reasons. The first one is that larger numbers of function bases increase the computational complexity with very modest improvements in the modeling accuracy; the second one is that a good initialization of the method requires n_c to be greater or equal to n_b.

- As anticipated in section 2.1, preparing for the developments shown in the next subsection, another requirement is needed for the set of function bases used to represent the free function: they must ensure the linear independence under the differential operators in equation(6), i.e., the resulting M matrix must be full rank. In this case, the requirement translates into omitting the function bases $h_j\big(z(x)\big)$ up to $j = 3$, leading to the following expression for the free function:

$$g(x) = \sum_{j=4}^{n_b} \xi_j h_j\big(z(x)\big)$$

Based on this consideration, the formulations for $\bar{h}\big(z(x)\big)$, $\bar{f}(x)$, $\bar{a}$, M, K can be obtained accordingly.

3.2. TFC-based Kalman Filter

In this subsection, the developments obtained up to now are applied to the problem of estimating the state of the system using a limited number of noisy measurements; the goal is reached by means of Kalman filter: we have just derived a linear finite-dimensional model for the dynamics of the structure that can be used for the process equation of the filter. Similarly for the measurement model, we will see that the constrained expression formulated before can provide a good answer to our needs.

As stated above, the TFC-based dynamic equation, represents an excellent process model to be used in the filter. The only thing that we need to do is to put equation (10) into a form that is more suitable for our purposes. To this aim, we can individuate an appropriate set of state variables transforming the equation from a set of second order ODEs to a set of first order ODEs; this can be achieved by simply considering the following augmented state vector:

$$\bar{\Xi} = \begin{bmatrix} \bar{\xi} \\ \dot{\bar{\xi}} \end{bmatrix}$$

Using this state variables, the state space matrix representation of the dynamical system will be:

$$\widetilde{M}\,\dot{\bar{\Xi}} + \widetilde{K}\,\bar{\Xi} = \bar{Q} \tag{11}$$

where we introduced the augmented matrices $\widetilde{M}$, $\widetilde{K}$:

$$\widetilde{M} = \left[\begin{array}{c|c} I_{n_b} & 0_{n_b \times n_b} \\ \hline 0_{n_c \times n_b} & M_{n_c \times n_b} \end{array}\right]$$

$$\widetilde{K} = \left[\begin{array}{c|c} 0_{n_b \times n_b} & -I_{n_b} \\ \hline K_{n_c \times n_b} & 0_{n_c \times n_b} \end{array}\right]$$

and the augmented input vector $\bar{Q}$:

$$\bar{Q} = \begin{bmatrix} 0_{n_b \times 1} \\ \hline \bar{q}(t) \end{bmatrix}$$

Choosing a linearly independent set of function bases, (10) (11) can be rewritten in the classic state space matrix form:

$$\dot{\bar{\Xi}} = A\,\bar{\Xi} + B\,\bar{Q} \tag{12}$$

where A, B are defined as follows:

$$A = -\big(\widetilde{M}^T\widetilde{M}\big)^{-1}\widetilde{M}^T\widetilde{K} \qquad B = \big(\widetilde{M}^T\widetilde{M}\big)^{-1}\widetilde{M}^T$$

Starting from this representation an equivalent discrete-time form of the system can be computed:

$$\bar{\Xi}_{k+1} = \hat{A}\,\bar{\Xi}_k + \hat{B}\,\bar{Q}_k \tag{13}$$

The next step consists in finding an appropriate measurement model that puts the actual stats of the system, that have no physical meaning in themselves, in relation to some measurable quantities that can be retrieved from sensors. The simplest choice for these measurements consists in the transversal displacements and displacement velocities of the beam at some points along the axis. Substituting the free function expansion in equation (8) into the constrained expression in equation (7), one gets an expression in terms of the free function coefficients that provides a map from the system states (i.e., the free function coefficients) to the physical displacements and displacement velocities of the beam. Exploiting this fact and writing the relation for all the n_s sample points, one can get the following measurement model to be used in the Kalman filter:

$$\begin{bmatrix} \bar{y} \\ \dot{\bar{y}} \end{bmatrix} = \widetilde{H}\,\bar{\Xi} \tag{14}$$

where $\bar{y}$, $\dot{\bar{y}}$ are the vectors with the n_c displacement and displacement velocity measurements.

The measurement model in equation (14) can be used to initialize the state estimate based on the first available measurement: this is accomplished by considering the sensor output at time t_0 and inverting the above equation. It is worth noting that the initial guess obtainable in this way brings the full and unattenuated measurement noise content with it.

Exploiting the fact that $\widetilde{H}$ is full rank (thus $\widetilde{H}^T\widetilde{H}$ is invertible), the initial estimate for the state is obtained as follows:

$$\bar{\Xi}_0 = \big(\widetilde{H}^T\widetilde{H}\big)^{-1}\widetilde{H}^T\begin{bmatrix} \bar{y}_0 \\ \dot{\bar{y}}_0 \end{bmatrix} \tag{15}$$

The last aspect of the problem we need to face, and usually one of the most challenging in the context of Kalman filtering, is the choice of the P_0, Q and R matrices, where P_0 is the initial value of the state estimate error covariance matrix P. In particular, the most difficult

to determine is the process noise covariance matrix and for this reason we will leave it as the last one.

Indeed, the choice of the R matrix is quite straightforward and most of the difficulties are related to the evaluation of the uncertainty in the measurements provided by the selected sensors. Obtaining this piece of information may require the modeling of the acquisition process and involve the geometry of the sensing system; moreover, depending on the case, this could lead to state-dependent or time-dependent R matrix, or both. In these cases, optimality and stability of the filter are not automatically guaranteed and the latter must be assessed for each operating condition by testing. However, the work presented in this paper is not aimed to investigate these aspects of the problem and a simple noise model with constant R was chosen for the implementation.

The initialization of the state error covariance matrix P is done by observing that the initial state estimate is obtained by using the measurements at time t_0, thus the covariance associated to this first guess can be computed directly from the sensor covariance matrix R.

$$R = \begin{bmatrix} \sigma_Y & | & 0_{n_c \times n_c} \\ --- & + & --- \\ 0_{n_c \times n_c} & | & \sigma_{\dot{Y}} \end{bmatrix} \tag{16}$$

$$P_0 = \left(\tilde{H}^T \tilde{H}\right)^{-1} \tilde{H}^T R \, \tilde{H} \left(\tilde{H}^T \tilde{H}\right)^{-1} \tag{17}$$

In the R formulation we are assuming that the displacement errors are uncorrelated to displacement velocity errors. In numerical tests we will further assume that displacement errors are uncorrelated to each other and the same for displacement velocity errors. This will make both σ_Y and $\sigma_{\dot{Y}}$ matrices diagonal.

As anticipated, the most challenging task is to compute the process noise covariance matrix P. This is of critical importance in the design of a Kalman filter since it accounts for all the uncertainties in the modeling of the system dynamics. These include both errors in the model parameters compared to their true values and unpredictable external disturbances or unmodeled dynamics; examples of this could be the small acceleration due to drag perturbations that may affect a vehicle otherwise moving with constant velocity. In this particular case, we can take advantage of a technique, developed by Abbeel et al. in [24], that allows to train the Q matrix comparing the predictions obtainable through the process model with reference values representing the true dynamics of the structure. The authors propose several techniques among which the most straightforward and convenient for this application is the approach that aims at maximizing the joint likelihood of the predictions according to this formula:

$$Q_{joint} = \arg\max_Q \left[-T \log|2\pi Q| - \sum_{k=1}^{T} \left(x_k - f(x_{k-1}, u_k)\right)^T Q^{-1} x_k - f(x_{k-1}, u_k)\right] \tag{18}$$

The problem has an explicit solution:

$$Q_{joint} = \frac{1}{T} \sum_{k=1}^{T} \left(x_k - f(x_{k-1}, u_k)\right)\left(x_k - f(x_{k-1}, u_k)\right)^T \tag{19}$$

This approach provides results in numerical simulations which are better than the ones obtainable by manually tuning the matrix and with a considerable time saving, as shown in [24]. The main issue is the need for a suitable set of reference values to be used to train the matrix. The problem is automatically solved when an analytical solution is available, but this is very unlikely in most cases. A very common approach is to use experimental data measured with high accuracy in very controlled environment; naturally, this kind of measurements are not generally obtainable with the same degree of accuracy in typical operating conditions, but it is not necessary, and moreover if that was possible the Kalman filter would be useless. In other words, the Q matrix training phase is needed to characterize the level of uncertainty of the results provided by the adopted theoretical model relative to the true dynamics.

In this work, we are going to replace the experimental data with a very accurate numerical propagation of the beam dynamics: this is consistent with the fact that the in the tests shown in the next section, the true behavior of the beam is simulated by numerical integration of the dynamic equation (6). As the results obtained in section 4 prove, this kind of approach provides a Q matrix that is capable to effectively represent the process noise even when the training is run considering the free response of the structure and the filter is then applied to the system subject to some forcing action.

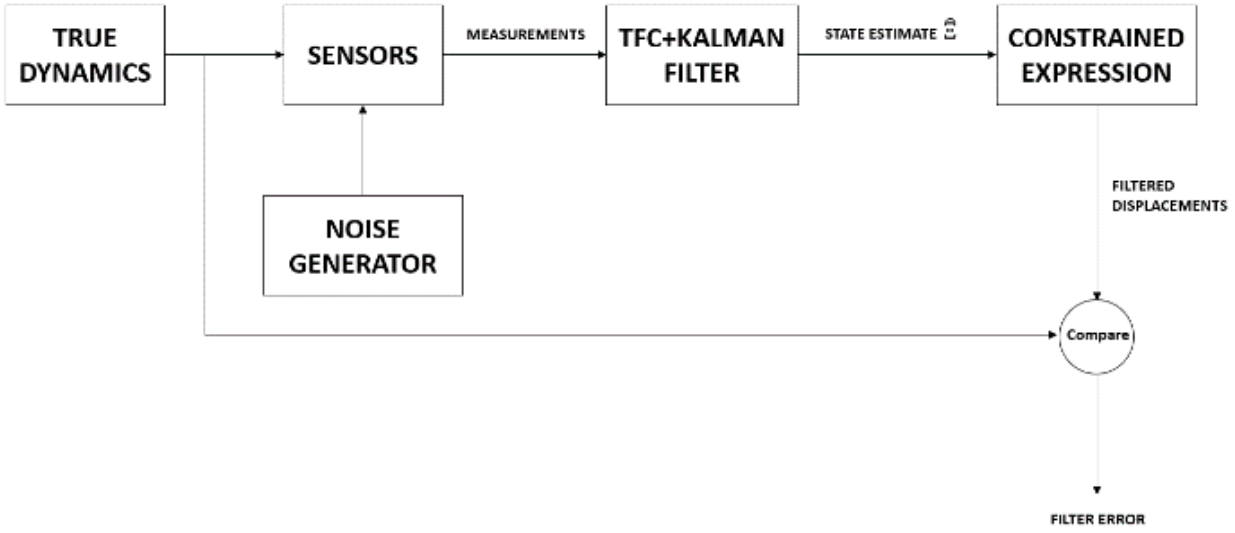

Figure 2- Numerical simulation setup

4. Numerical Simulation and Results

In the following, the method presented above is tested based on numerical simulations and the results are shown. The section is divided into 2 subsections: in the first one the simulation setup adopted for the different tests is thoroughly described, while in the second one the results are presented and commented.

4.1. Simulation Setup

In Figure 2 a diagram representing the simulation workflow is reported. The true displacements and displacement velocities of the beam are computed and used as the ground truth needed to assess the filter performance; then the available measurements are simulated starting from the simulated dynamics and some error is added based on the chosen noise model. The application of the Kalman filter is the next step, carried out using the noisy measurements obtained so far: the output is the estimated state vector $\hat{\Xi}$ that, as explained in the model description, does not correspond to any physical measurement; thus, one further step is required to transform the filter output to displacement and displacement velocity estimates that can be compared to the ground truth to evaluate the filtering performance: this can be conveniently done by using the constrained expression itself, as represented in equation (7) .The actual dynamics of the structure are simulated by direct numerical integration of the equation (6) using highly accurate methods and tolerances. In particular, the solver developed for this problem is based on the technique presented by Jacquot and Dewey in [25]. The integration is quite time-consuming using high precision settings, but this is not a problem for the simulation, since the ground truth can be computed offline and does not affect the filter performance evaluation.

In the test campaign, the sensors are assumed to directly measure the displacements and velocities at some locations along the beam axis (see Figure 1 for reference) and the noise model is very simple and characterized by the following parameters:

$$\begin{cases} \mu_{y_{err}} = 0\ m \\ \mu_{\dot{y}_{err}} = 0\ m/s \\ \sigma^2_{y_{err}} = 0.01\ m \\ \sigma^2_{\dot{y}_{err}} = 0.005\ m/s \end{cases}$$

where μ denotes the mean of the error distribution and σ^2 its variance.

4.1.1. Performance Metrics

The accuracy performance of the filter is evaluated by considering the following metrics:

- Mean error time history computed along the whole beam span: this represents the time evolution of the average of the estimation errors at the available measurement points along the beam.

$$\mu_\epsilon(k\Delta t) = \frac{1}{n_c}\sum_{i=1}^{n_s}\left(\hat{y}_i(k\Delta t) - \bar{y}_i(k\Delta t)\right) \qquad (20)$$

Here $\hat{y}_i(t)$ denotes the estimate at time t and position x_i, while $\bar{y}_i(t)$ is the true value at time t and position x_i . The statistics are

computed for both the displacement and the displacement velocity.

- Time history of the error standard deviation computed along the whole beam span: the approach is totally analogous to the one followed for the mean and it uses the following definition for the sample standard deviation:

$$\mu_\epsilon(k\Delta t) = \sqrt{\frac{1}{n_c - 1}\sum_{i=1}^{n_s}\left(\epsilon_i(k\Delta t) - \mu_\epsilon(k\Delta t)\right)^2} \quad (21)$$

where $\epsilon_i(k\Delta t)$ is the estimation error at the station x_i

$$\epsilon_i(k\Delta t) = \hat{y}_i(k\Delta t) - \bar{y}_i(k\Delta t) \quad (22)$$

- Free tip displacement time history: the free tip of a cantilever beam is often the part subject to the widest excursion, thus the time evolution of its displacement is recorded and compared to the ground truth to have a significant insight on the actual performance of the Kalman filter. Finally, the plots relative to this metric include the corresponding noisy measurements time history for a better performance assessment.

4.1.2. Physical Model Parameters

The simulated structure is a simple cantilever beam and the mechanical and geometrical parameters describing its dynamics do not change through the different tests. What follows is a summary of this information:

$$\begin{cases} E = 70.00\ GPa \\ \rho = 2700\ kg/m^3 \end{cases} \qquad \begin{cases} L = 1.000\ m \\ A_s = \pi \times 10^{-4}\ m^2 \\ I = 7.854 \times 10^{-9}\ m^4 \end{cases}$$

4.1.3. Q Matrix Training

The technique used to obtain the process noise covariance matrix Q is the one described in subsection 3.2 and, in greater detail in [24]. In the numerical simulation framework, the set of high-accuracy experimental measurements used to compute the Q matrix by comparison with the predictions provided by the filter process model are represented by the simulated ground truth (i.e., the structure dynamics obtained by numerical integration of equation (6)). In order to assess the capability of this method to ensure the convergence of the filter in a variety of different conditions without requiring a specific training for each of them, the Q matrix will be computed only once using as a reference the simple free response of the structure under an initial condition that will not be used in any of the actual tests. Considering that the first natural frequency of the system is $14.247\ Hz$ (it can be computed by solving the TFC-based model associated eigenvalue problem in a faster and easier way than going through the classic approach for the PDE), a training time interval of 1 second is considered sufficient to gather enough information to compute an effective covariance matrix. The training conditions are reported in Table 2:

Table 2 – Conditions for training the Kalman filter covariance matrices.

TRAINING CASE	
Forcing	none (free response)
Training time interval	$1\ s$
Initial condition for training	Static deformed shape under a tip load of $P = 100\ N$

4.2. Results

Results of the simulations carried out using the models and parameters presented in the above subsection are now shown. Firstly, the results obtained considering the free dynamics of the system are shown, then a forcing action is included in the simulation and the performance of the TFC-based Kalman filter is assessed.

4.2.1. Simulation with free response

The first test whose results we are going to present is the free response of the beam subject to the initial conditions reported in Table 3.

Table 3 - Initial condition for the free response of the beam.

INITIAL CONDITION	
Description	Static deformed shape under a tip load of $P = 50\ N$
Formula	$y(x,0) = \frac{Px^2}{6EI}(3L - x)$ $\dot{y}(x,0) = 0$

This and all the other simulations were run for $10\ s$, which, based on the natural frequency of the dynamics, is a sufficiently long time interval. Despite this, if significant changes do not occur from a certain time on (e.g., when the error statistics have reached a steady-state), the stationary part will be omitted in the plots to allow a better focus on the most meaningful time interval. The propagation time step used to simulate the true dynamics of the structure is $0.001\ s$, since it can be small as desired and should guarantee a high numerical accuracy to the simulation. Finally, for the free response

test, the process equation discretization time step is set to $0.01\ s$.

The fast filter convergence is clearly noticeable in Figure 3 and Figure 4. A short increase in both the mean error and its variance occurs during the very first time instants and then these statistics quickly reduce to small values. Similar results can be appreciated looking at the free tip actual/estimated displacement plots in Figure 5 and Figure 6; moreover, it can be noted that the accuracy of the estimation is limited by the filter time step that is significantly larger than the one used to simulate the true dynamics (in this case it is 1 order of magnitude larger): this also explains the steady-state fluctuations in the estimation error, being the filter accuracy in average better when the actual displacement is distant from maxima/minima.

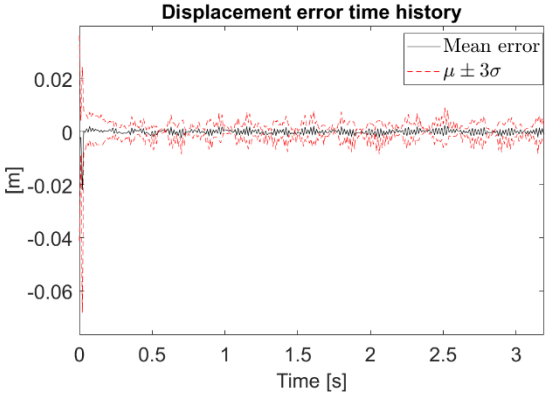

Figure 3 - Average displacement estimation error time evolution. Test case: beam free response ($\Delta t = 0.01s$). 3σ limits are reported as well.

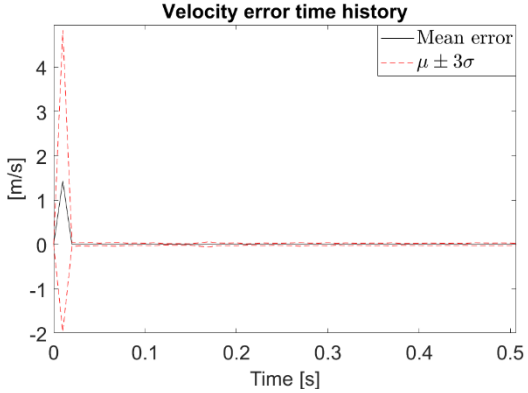

Figure 4 - Average displacement velocity estimation error time evolution. Test case: beam free response ($\Delta t = 0.01s$). 3σ limits are reported as well.

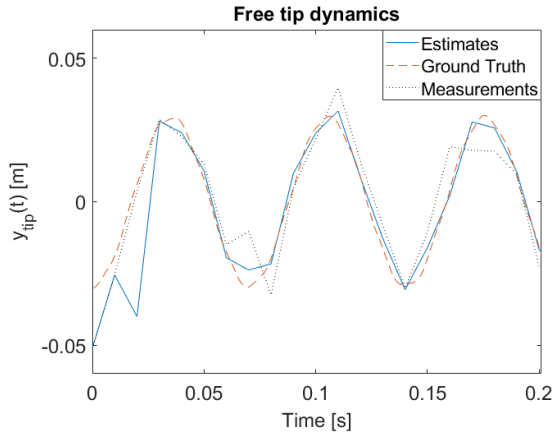

Figure 5 - Beam free tip displacement estimation. Test case: beam free response ($\Delta t = 0.01s$). Detail of the first simulated time instants.

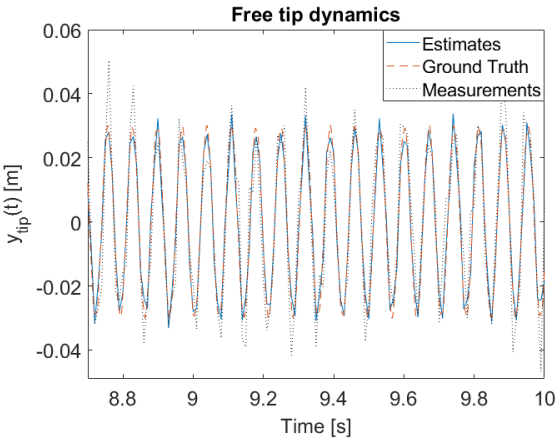

Figure 6 - Beam free tip displacement estimation. Test case: beam free response ($\Delta t = 0.01s$). Detail of the last simulated time instants.

4.2.2. Simulation with forced response

In the previous paragraph, the effect of the size of the time step on the accuracy of the state estimate was highlighted. In the following, we are going to show that impact of the time step used to run the filter is even more significant when dealing with some inputs to the system dynamics. To this end, a cosine forcing input at the free tip was simulated with the following characteristics:

$$F(x,t) = \begin{cases} F_0 \cos(2\pi f t) & x = L \\ 0 & x \neq L \end{cases}$$

The amplitude of the forcing is $F_0 = 15\ N$, while the frequency was chosen $f = 5\ Hz$ to be far away from the resonance condition of the structure and at the same time not in the higher frequency region since that would require a high sampling frequency to correctly track the dynamics of the beam.

The adoption of this last precaution still does not allow to effectively use the same process equation discretization time step $\Delta t = 0.01\,s$ used in previous simulation and obtain good results. Reducing instead to $\Delta t = 0.005\,s$, the performance shown in Figure 7 and Figure 8 is achieved.

Looking at Figure 9, one can notice that the initial settling of the estimate is more difficult with a much larger error and a longer time required to match the actual state of the system compared to what happens in Figure 5. Finally, Figure 10 shows that the filter accuracy at the steady state is reduced due to its inability to track the true displacement with high accuracy: this is related to the presence of some higher frequency oscillations that cannot be adequately sampled using the chosen time step.

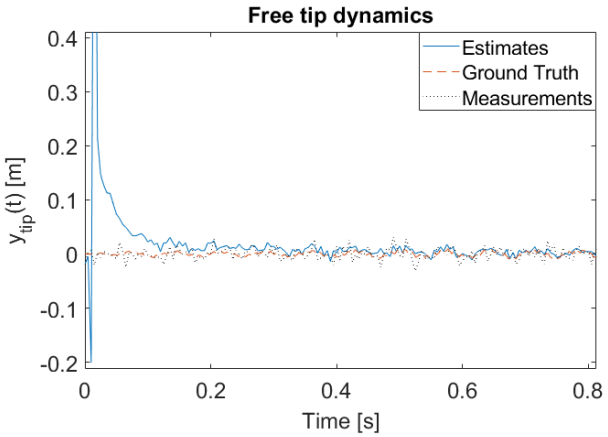

Figure 9 - Beam free tip displacement estimation. Test case: beam cosine forced response ($\Delta t = 0.005s$). Detail of the first simulated time instants.

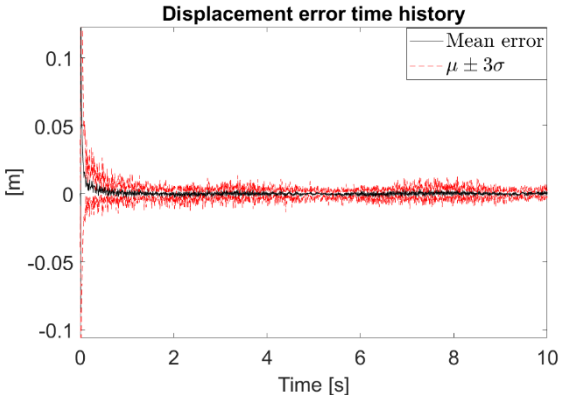

Figure 7 - Average displacement estimation error time evolution. Test case: beam cosine forced response ($\Delta t = 0.005s$). 3σ limits are reported as well.

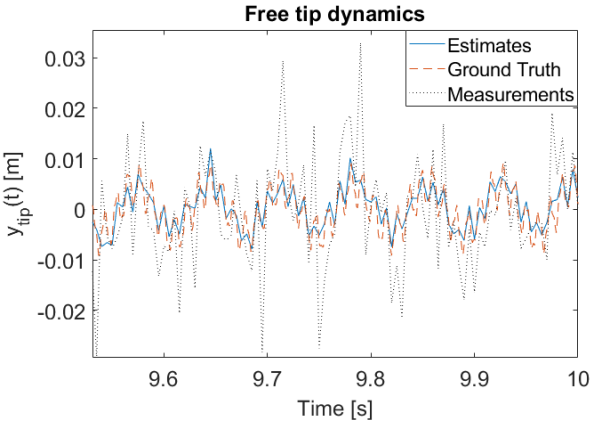

Figure 10 - Beam free tip displacement estimation. Test case: beam cosine forced response ($\Delta t = 0.005s$). Detail of the last simulated time instants.

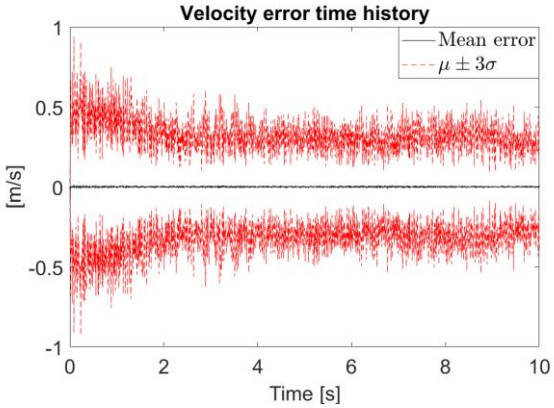

Figure 8 - Average displacement velocity estimation error time evolution. Test case: beam cosine forced response ($\Delta t = 0.005s$). 3σ limits are reported as well.

A proof of the effectiveness of the model is found by reducing the time step to $\Delta t = 0.001\,s$. The results obtained with this time discretization are reported in Figure 11, Figure 12, Figure 13 and Figure 14. In particular, in Figure 13 and Figure 14 the better convergence obtained by the filter can be observed.

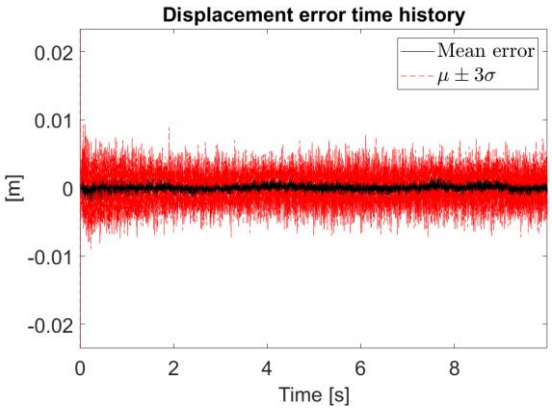

Figure 11 - Average displacement estimation error time evolution. Test case: beam cosine forced response ($\Delta t = 0.001s$). 3σ limits are reported as well.

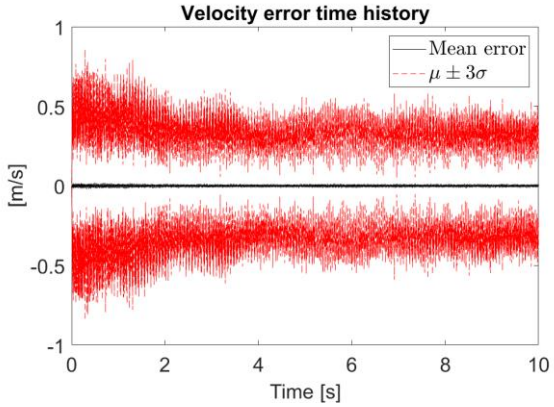

Figure 12 - Average displacement estimation error time evolution. Test case: beam cosine forced response ($\Delta t = 0.001s$). 3σ limits are reported as well.

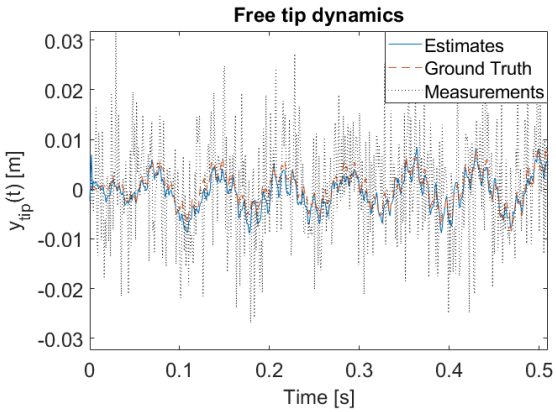

Figure 13 - Beam free tip displacement estimation. Test case: beam cosine forced response ($\Delta t = 0.001s$). Detail of the first simulated time instants.

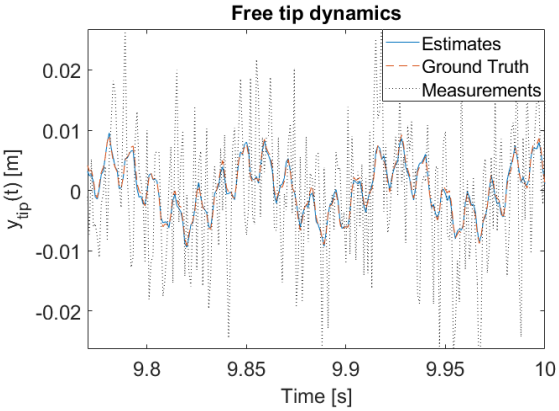

Figure 14 - Beam free tip displacement estimation. Test case: beam cosine forced response (Δt=0.001s). Detail of the last simulated time instants.

In this section, the results of the tests carried out to assess the effectiveness of the developed method were shown. The Kalman filter based on the TFC model was tested for the structure under different conditions. In particular, the method has proved to provide good estimates of the true state of the system both when the structure is freely vibrating because of an initial deformed condition and when it is responding to an external input, like a force applied to the free tip. As expected, the frequency at which the filter is run has an impact on the performance. In particular, this aspect becomes critical when the filter is applied to track the response of the system to a periodic forcing action because of the possibility of the input to excite higher frequency modes of the structure. In the special case of a tip load input that follows a low-frequency cosine time law, a time step that is significantly smaller than to the one adopted in the case of the free-response proved to be necessary to get a similar performance.

5. Conclusions

In this work the development of a novel technique for modeling the dynamics of a distributed flexible system using a finite number of state variables was shown. The proposed method exploits the TFC framework to mathematically represent the structure under consideration and all the constraints acting on it.

Then, a Kalman filter implementation was developed based on that model. The special case of the Euler-Bernoulli beam dynamics was chosen to provide an application example that is simple enough to not hide the key concepts of the proposed methodology. Since the PDE governing the dynamics of the system is linear, the resulting TFC-based model is linear as well. This leads to the implementation of a linear Kalman filter for the estimate of the state of the system.

Finally, the effectiveness of the developed method was tested by means of numerical simulations.

The advantage of the proposed approach is twofold. On one side the dimensionality of the problem is reduced from infinite to a finite number of time-dependent state variables that, using methods like the orthogonal polynomials expansion exploited in this paper, can be kept reasonably small. The consequence of this is that the resulting dynamical model can be used to predict, estimate and control the state of the system in a way that is reliable and simpler than when dealing with infinite-dimensional representations. On the other hand, the TFC-based approach allows for a simpler modeling procedure by removing the need for the designer to choose the approximating functions based on previous knowledge or on tedious and time-demanding analyses: once the basics of the method are clear, the entire procedure can be automatized while still leaving the user with a certain degree of freedom in balancing complexity and accuracy of the resulting model. The choice of applying this novel approach to a simple structure aimed at preventing a higher complexity from hiding the key features of the proposed method. Anyway, the applicability of this approach is not specially limited by the complexity of the mechanical model. There are no simplification requirements in the derivation of the dynamic equations and structures based on more complex models can still be treated following the logic and the principles presented above. The only difference will be in the amount of work required and in the complexity of the resulting mathematical representation. In this way, nonlinear structural dynamics can be modeled using the TFC as well. Then, the resulting TFC-based nonlinear model can be used with an EKF or an UKF to estimate the dynamics of such systems. Finally, another extension of the method presented in this paper that is worthy of further investigations is the application to structures that cannot be considered as one-dimensional.

Acknowledgements
The authors thank the Air Force Office of Sponsor Research for supporting this investigation under the grant #FA9550-22-1-0104.

References

[1] V. Akan, E. Yazgan and A. Sabban, "Antennas for space applications: A review," in *Advanced Radio Frequency Antennas for Modern Communication and Medical Systems*, IntechOpen UK, 2020, pp. 139-171.

[2] M. Touratier, "An efficient standard plate theory," *International journal of engineering science*, vol. 29, no. 8, pp. 901-916, 1991.

[3] J. Junkins, Introduction to dynamics and control of flexible structures, Aiaa, 1993.

[4] T. Meurer, "Some perspectives in PDE control," in *Proc. 20th IFAC World Congress*, 2017.

[5] S. Peitz, J. Stenner, V. Chidananda, O. Wallscheid, S. L. Brunton and K. Taira, "Distributed Control of Partial Differential Equations Using Convolutional Reinforcement Learning," *arXiv preprint arXiv:2301.10737*, 2023.

[6] S. L. Brunton, B. R. Noack and P. Koumoutsakos, "Machine learning for fluid mechanics," *Annual review of fluid mechanics*, vol. 52, pp. 477-508, 2020.

[7] B. O. Al-Bedoor and Y. A. Khulief, "Finite element dynamic modeling of a translating and rotating flexible link," *Computer methods in applied mechanics and engineering*, vol. 131, no. 1-2, pp. 173-189, 1996.

[8] K.-J. Bathe, Finite element procedures, Klaus-Jurgen Bathe, 2006.

[9] J. N. Reddy, An introduction to the finite element method, McGraw-Hill Education, 2019.

[10] P. Gasbarri, R. Monti, C. de Angelis and M. Sabatini, "Effects of uncertainties and flexible dynamic contributions on the control of a spacecraft full-coupled model," *Acta Astronautica*, vol. 94, no. 1, pp. 515-526, 2014.

[11] J. L. Junkins and Y. Kim, "Assumed Modes Method," in *Introduction to Dynamics and Control of Flexible Structures*, Washington DC, American Institute of Aeronautics and Astronautics, 1993, pp. 185-189.

[12] R. E. Kalman, "A new approach to linear filtering and prediction problems," 1960.

[13] S. F. Schmidt, "The Kalman filter-Its recognition and development for aerospace applications," *Journal of Guidance and Control*, vol. 4, no. 1, pp. 4-7, 1981.

[14] M. I. Ribeiro, "Kalman and extended kalman filters: Concept, derivation and properties," *Institute for Systems and Robotics*, vol. 43, no. 46, pp. 3736-3741, 2004.

[15] E. A. Wan and R. van der Merwe, "The unscented Kalman filter for nonlinear estimation," in *Proceedings of the IEEE 2000 Adaptive Systems for Signal Processing, Communications, and Control Symposium (Cat. No.00EX373)*, 2000.

[16] R. Curtain, "A Survey of Infinite-Dimensional Filtering," *Siam Review,* vol. 17, no. 3, pp. 395-411, 1975.

[17] X. Wu, B. Jacob and H. Elbern, "Optimal control and observation locations for time-varying systems on a finite-time horizon," *SIAM Journal on Control and Optimization,* vol. 54, no. 1, pp. 291-316, 2016.

[18] S. Afshar, F. Germ and K. Morris, "Well-posedness of extended Kalman filter equations for semilinear infinite-dimensional systems," in *2020 59th IEEE Conference on Decision and Control (CDC)*, 2020.

[19] C. Leake, H. Johnston and D. Mortari, The Theory of Functional Connections, Lulu.com, 2022.

[20] D. Mortari, "The theory of connections: Connecting points," *Mathematics,* vol. 5, no. 4, p. 57, 2017.

[21] D. Mortari and C. Leake, "The Multivariate Theory of Connections," *Mathematics,* vol. 7, no. 3, p. 296, 2019.

[22] H. Johnston and D. Mortari, "Linear Differential Equations Subject to Multivalued, Relative and/or Integral Constraints with Comparisons to Chebfun," *SIAM Journal of Numerical Analysis,* 2018.

[23] C. Leake and D. Mortari, "An Explanation and Implementation of Multivariate Theory of Connections via Examples," in *Proceedings of the AIAA/AAS Astrodynamics Specialist Conference*, Portland, ME, USA, 2019.

[24] P. Abbeel, A. Coates, M. Montemerlo, A. Y. Ng and S. Thrun, "Discriminative training of Kalman filters," in *Robotics: Science and systems*, 2005.

[25] R. Jacquot and B. R. Dewey, "Solution of static and dynamic beam bending and static buckling problems using finite differences and MATLAB," in *2001 Annual Conference*, 2001.

[26] R. E. Kalman, "A new approach to linear filtering and prediction problems," *ASME - Journal of Basic Engineering,* vol. 82, no. D, pp. 35-45, 1960.